HHS Public Access

Author manuscript

J Control Release. Author manuscript; available in PMC 2016 December 14.

Published in final edited form as:

J Control Release. 2015 December 28; 220(Pt B): 592–599. doi:10.1016/j.jconrel.2015.08.033.

Spatiotemporal drug delivery using laser-generated-focused ultrasound system

Jin Di[a,c,1], **Jinwook Kim**[b,1], **Quanyin Hu**[a,c], **Xiaoning Jiang**[b,*], and **Zhen Gu**[a,c,d,**]

[a]Joint Department of Biomedical Engineering, University of North Carolina at Chapel Hill and North Carolina State University, Raleigh, NC 27695, USA

[b]Department of Mechanical and Aerospace Engineering, North Carolina State University, Raleigh, NC 27695, USA

[c]Center for Nanotechnology in Drug Delivery and Division of Molecular Pharmaceutics, UNC Eshelman School of Pharmacy, University of North Carolina at Chapel Hill, Chapel Hill, NC 27599, USA

[d]Department of Medicine, University of North Carolina at Chapel Hill, Chapel Hill, NC 27599, USA

Abstract

Laser-generated-focused ultrasound (LGFU) holds promise for the high-precision ultrasound therapy owing to its tight focal spot, broad frequency band, and stable excitation with minimal ultrasound-induced heating. We here report the development of the LGFU as a stimulus for promoted drug release from microgels integrated with drug-loaded polymeric nanoparticles. The pulsed waves of ultrasound, generated by a carbon black/polydimethylsiloxane (PDMS)-photoacoustic lens, were introduced to trigger the drug release from alginate microgels encapsulated with drug-loaded poly(lactic-co-glycolic acid) (PLGA) nanoparticles. We demonstrated the antibacterial capability of this drug delivery system against *Escherichia coli* by the disk diffusion method, and antitumor efficacy toward the HeLa cell-derived tumor spheroids *in vitro*. This novel LGFU-responsive drug delivery system provides a simple and remote approach to precisely control the release of therapeutics in a spatiotemporal manner and potentially suppress detrimental effects to the surrounding tissue, such as thermal ablation.

Keywords

Drug delivery; Photoacoustic; Nanoparticles; Microgels; Stimuli responsive

1. Introduction

Development of remotely controlled drug release techniques for noninvasive and spatiotemporal administration has attracted increasing attentions these years [1–3]. To date,

*Corresponding author. xjiang5@ncsu.edu (X. Jiang). **Correspondence to: Z. Gu, Joint Department of Biomedical Engineering, University of North Carolina at Chapel Hill and North Carolina State University, Raleigh, NC 27695, USA. zgu@email.unc.edu (Z. Gu).

[1]These authors contributed equally to this work.

a variety of external stimuli have been employed, such as thermal, electric, magnetic, optical excitations and ultrasound [2,4,5]. Owing to its ease of administration, the high-intensity-focused ultrasound (HIFU)-triggered drug delivery system is of particular interest for locally on-demand delivery of therapeutic agents, including proteins, peptides and small molecular drugs [6–9]. The promoted release effects can be attributed to one or combinations of four mechanisms: cavitation, radiation pressure, acoustic streaming, and ultrasound-induced heating [10–14]. Among these mechanisms, the thermal ablation can damage the surrounding tissues [7]. Hence, a precise control for the localized drug release at a tight focal spot with relatively low acoustic power and duty cycle is required to suppress the detrimental effects to the surrounding tissue.

Recently, a laser-generated focused ultrasound (LGFU) transducer has been developed to realize a high-frequency focused ultrasound with a tight focal spot (<1 mm) and low duty cycle (<0.001%). The transducer is comprised of a concave glass coated with a laser-absorption layer made from carbon-nanotube and a thermal-expansion layer with a high thermal expansion coefficient such as polydimethylsiloxane (PDMS) [15]. In comparison with the conventional HIFU, LGFU shows several advantages, including 1) relatively high frequency (>10 MHz) that achieves a tight focal spot for ultrasound therapy; 2) small aperture for precise control of the acoustic cavitation; and 3) the reduced ultrasound-induced heating due to the very low duty cycle (a single-pulsed wave with a pulse repetition rate of 10 to 20 Hz) [16]. We hypothesize that such merits of LGFU could provide an efficacy for the remote and spatiotemporal control of the drug release with a high resolution without detrimental effects to the surrounding tissue. Herein, we utilized the LGFU as a trigger for promoting drug release from a formulation comprised of alginate sphere microgels integrated with drug-loaded poly(lactic-co-glycolic acid) nanoparticles (PLGA NPs). As depicted in Fig. 1, a LGFU transducer is composed of a plano-concave glass lens coated with a layer of carbon-black/PDMS composite. The pulsed laser energy is absorbed by the carbon black particles and subsequently heats the surrounding elastomeric polymer. The rapidly transferred thermal energy causes instantaneous thermal expansion of the PDMS layer which can generate a high-frequency (>10 MHz), high-amplitude (>10 MPa) pulsed wave. Once the laser-generated-pulsed waves excite the microgels, cavitation effects at the microgels and oscillation of the microgels' shells promote the release of the drug gradually released from PLGA NPs and temporarily stored in the microgels.

2. Materials and methods

2.1. Materials

PLGA (actide:glycolide (50:50), MW: 40–75 kDa), anhydrous dichloromethane (DCM), sodium alginate, barium chloride dihydrate, 1,6-diaminohexane, *N*-(3-dimethylaminopropyl)-*N*′-ethylcarbodiimide hydrochloride (EDC), *N*-hydroxysulfosuccinimide sodium salt (NHSS), fluorescein isothiocyanate (FITC, isomer I) and ciprofloxacin (CIF) were obtained from Sigma Aldrich (St. Louis, MO). Doxorubicin hydrochloride (DOX) was obtained from Fisher Scientific (Pittsburgh, PA). The deionized (DI) water was prepared by a Millipore NanoPure purification system (resistivity higher than 18.2 $M\Omega \cdot cm^{-1}$). All chemicals were reagent grade and used as received.

For the LGFU transducer, a plano-concave lens with a diameter of 12 mm and a radius of curvature of 12.4 mm (Edmund optics Inc., Barrington, NJ) was used as a transparent substrate. Commercial carbon black powders (Carbon black 73116, Acrylicos Vallejo, Barcelona, Catalonia, Spain) were mixed with PDMS solution (Sylgard 184, Dow Corning Corporation, Midland, MI) and coated onto the curved surface as the light absorption and thermoelastic layer [17].

2.2. Preparation and characterization of the drug loaded PLGA NPs

The DOX and CIF loaded PLGA NPs were prepared *via* a double-emulsion method [6]. Briefly, 4.5 mL organic phase DCM containing 180 mg PLGA was emulsified with 0.5 mL aqueous phase containing 5 mg DOX and 15 mg CIF, respectively, followed by sonication for 40 cycles (1 s each with a duty cycle of 40%), and then the primary emulsion was immediately poured into 25 mL 1 wt.% alginate aqueous solution and then followed by the same sonication procedure. The double emulsion was subsequently transferred into 150 mL 0.2 wt.% alginate aqueous solution. The mixed suspension was stirred at room temperature for 2 h to eliminate DCM by evaporation. The resulted NPs were washed and collected by repeating the procedures of centrifuging at 10,000 rpm and suspending in DI water three times. The particle size and polydispersity intensity were measured by dynamic light scattering (DLS). The zeta potential of the NPs was determined by their electrophoretic mobility using the same instrument after appropriate dilution in DI water. Measurements were made in triplicate at room temperature. NPs morphologies were investigated by a scanning electron microscopy (SEM) (JEOL 6400 F, Tokyo, Japan) operated at 20 kV. The encapsulation efficiency (*EE*) and loading capacity (*LC*) of Doxorubicin (DOX) and ciprofloxacin (CIF) in NPs were calculated using the equations given below ($n = 3$).

$$EE\,(\%) = \frac{\text{Amount of drug in the nanoparticles}}{\text{Total amount of drug in dispersion}} \times 100\% \quad (1)$$

$$LC\,(\%) = \frac{\text{Amount of drug in the nanoparticles}}{\text{Nanoparticles' weight}} \times 100\% \quad (2)$$

2.3. Synthesis of FITC-alginate derivative

120 mg Sodium alginate was reacted with 1-ethyl-3-(3-dimethylaminopropyl)carbodiimide (EDC)/*N*-hydroxysuccinimide (NHS) (50 mg/30 mg) for activation of carbonyl groups of alginate in sodium buffer (pH = 5.0) for 30 min, followed by additional 1,6-diaminohexane (60 mg) for 4 h. The mixture was precipitated in 2-propanol (IPA) to remove unreacted diamine. The alginate-amine derivative was reacted with FITC (0.5 mg) in sodium bicarbonate solution (50 mM; pH = 8.5) for 4 h and precipitated in acetone to remove the unreacted FITC [18]. The resulting FITC-alginate derivative was dissolved in DI water. Labeled alginate was mixed with 50 g of 2 wt.% unlabeled sodium alginate solution and then the mixture was made into microspheres using the following process.

2.4. Preparation and characterization of alginate microgels loaded with drug containing PLGA NPs

Drug loaded PLGA NPs were added and thoroughly mixed with the 2 wt.% alginate solution. The weight ratio of alginate/PLGA/DOX was 1/90/2.5 and alginate/PLGA/CIF was 1/90/7.5. The homogeneous mixture was vacuumed for 30 min before transferring into a 5 mL syringe with an attached blunt tip, 22 gauge metal needle. The syringe was placed in an electrospray system equipped with a syringe pump. The positive electrode of the electrospray system was connected to the needle, and the negative electrode was connected to a metal receiving container with 50 mL of 20 mM $BaCl_2$. The solution was sprayed at a 0.155 mL/min flow rate under a high voltage (8 kV) and a working distance of 5 cm to the receiving container. The particles were cross-linked by 20 mM $BaCl_2$ bath solution for 5 min. The collected alginate microgels were then rinsed three times with DI water by successive centrifugation cycles and stored at 4 °C after lyophilization.

5.0% (w.t.) of the FITC alginate derivative was added into the 2 wt.% alginate solution for imaging by the laser scanning confocal microscopy (LSCM) (Zeiss LSCM 710, Carl Zeiss Micro Imaging, NY, USA). Alginate microgel sizes were determined by measuring the size of the particles under an optical microscope. The structure of NPs loaded microgels was characterized using scanning electron microscope (SEM). To prepare SEM samples, microgels were initially suspended in DI water. After dispersion, the microgels were dehydrated in a series of ethanol solutions (20%, 40%, 60%, 80%, 90%, 95%, 100%) and then sputter-coated with gold/palladium. The LSCM was used to visualize FITC-labeled alginate microgel loaded with NPs (encapsulated with DOX). Sections of the confocal two-dimensional (2D) slice images were generated from the top to the depth of 100 μm for each specimen. Afterwards, ZEN software (Carl Zeiss MicroImaging, NY, USA) was used to reconstruct the three-dimensional (3D) images [19].

2.5. Fabrication and characterization of the LGFU lens

The above mentioned plano-concave lens was spin-coated (3000 rpm) with a carbon-black/PDMS mixture (70% mass concentration of the carbon-black powder) and cured at 65 °C for 2 h. The excitation laser source is a 532 nm Q-switched Nd:YAG pulsed laser (SL-III-10, Continuum, San Jose, CA) with a pulse duration of 6 ns and a pulse repetition frequency of 10 Hz. A needle hydrophone (HNA-0400, Onda Corp., Sunnyvale, CA) was positioned at the focal distance of the LGFU lens in a water tank for acoustic field measurements. The input laser energy was controlled from 1 mJ to 6.5 mJ, and the corresponding peak-to-peak acoustic pressure output was measured. Due to the measurement limit of the hydrophone (~4 MPa negative pressure), the pressure outputs at 3 mm away (in the axial direction) from the focal distance were measured while increasing the laser energy up to 18 mJ. Since the pressure output profile is determined by the *f*-number (defined as the ratio of the radius of the curvature to the lens diameter) of the LGFU lens [15,20], the pressure output at the focal distance was indirectly characterized by considering a focal gain.

2.6. Drug release test

The drug-formulated alginate microgels were immersed in 500 μL phosphate buffered saline (PBS) solution in a 1.5 mL test tube. The microgels in the test tubes were treated by LGFU,

then the supernatant was collected and tested after centrifuging at 1500 rpm for 2 min. The amount of released DOX was measured by fluorescence (λ_{ex} = 470 nm, λ_{em} = 590 nm) using the same microplate reader. For quantitative analysis of CIF samples, the released CIF suspension was pipetted into a UV-transparent microplates (Corning® 96 well plates, Sigma-Aldrich), then the absorbance of the plates was read at 277 nm using the microplate reader. In order to check the temperature variation during the LGFU treatment (18 mJ, 5 min), temperature inside of one test tube with microgels loaded with DOX-NPs was monitored using needle thermocouple probe (HYP0, Omega Engineering Inc., Stamford, CT).

2.7. Anti-proliferation test

The anti-proliferation activity of the DOX-formulated microgels on HeLa cells was evaluated by using the 3-(4,5-dimethylthiazol-2-yl)-2,5-diphenyltetrazolium bromide (MTT) assay. Briefly, the cells were seeded in 96-well plates at the density of 7.5×10^3 cells/well. When the cells reached 70–80% confluence, 50 μL of released media were collected from the DOX-formulated either with or without LGFU treatment and then added to each well. Before the addition of the collected solution, the cells were washed by PBS, followed by adding 150 μL of FBS (fetal bovine serum) free medium and additional 20 μL of fresh made MTT solution (5 mg/mL). After 4 h of incubation, the media were carefully removed and 150 μL of dimethylsulfoxide (DMSO) were added, the plates were subjected to a microplate reader for cell viability assay at the wavelength of 570 nm with a reference wavelength at 690 nm within 10 min.

2.8. HeLa spheroids growth inhibition

HeLa spheroids were prepared by a lipid overlay method as reported by Hu et al. [21] Briefly, a 48-well plate was initially coated with 2% (w/v) agarose gel to prevent cell adhesion. After that, HeLa cells were seeded into each well at a density of 2×10^3 cells/well, and then incubated at 37 °C for 7 days to achieve a uniform and compact multicellular spheroids structure.

For evaluation of the anti-growth ability of DOX-formulated microgels on HeLa spheroids, the selected HeLa spheroids (7 days of incubation) were exposed to 50 μL collected solution from samples after LGFU treatment. As shown in Fig. 3A, after the microgel solution was exposed to the LGFU, the collected supernatant solution (50 μL) was applied on the selected HeLa spheroids. 50 μL-solution collected from without LGFU treatment were included for comparison and the spheroids incubated with drug-free Dulbecco's Modified Eagle's Medium (DMEM) were used as the negative control. After 3 days, 5 days and 7 days, the anti-growth efficacy against HeLa spheroids was evaluated by measuring the size of HeLa spheroids under an invert microscope (Olympus IX71, Shinjuku, Tokyo). All experiments were performed in triplicate.

2.9. Antibacterial effect

The disk diffusion method was used to assess the bactericidal capability of the sample solutions. Briefly, 50 μL of sample solution was collected after LGFU treatment and then dropped to a sterilized filter-paper disk (diameter: 5 mm), dried at room temperature, and

then introduced an agar plate already inoculated with *Escherichia coli* (ATCC 25922, seeding density of 5×10^3 cells/cm^2). After incubating for 24 h at 37 °C, the diameters of the transparent inhibitory zone produced around the paper disk were measured.

2.10. Statistical analysis

All results presented were averaged and expressed as the mean ± SD. Student's *t*-test or ANOVA were utilized to determine statistical significance between different groups. A P value < 0.05 was considered to be statistically significant.

3. Results and discussion

3.1. Characterization of the PLGA NPs

The drug-loaded PLGA NPs were prepared through a w/o/w double emulsion–solvent-evaporation method [22]. The particle sizes of DOX-formulated NP and CIF-formulated NP were 249.2 ± 10.1 nm and 259.9 ± 17.2 nm, respectively (Table 1). The zeta potential of DOX-formulated NP and CIF-formulated NP were −67.2 ± 5.1 mV and −65.5 ± 4.3 mV, respectively. The size distribution and morphology of PLGA NPs were shown in Fig. 2A. The PLGA NPs exhibited the uniform spherical shape under SEM, and encapsulation of DOX or CIF did not significantly change the particle size. The LC of DOX-formulated NP and CIF-formulated NP was 3.3 ± 0.2% and 3.5 ± 0.3% respectively, with the EE of 47.3 ± 7.1% and 44.3 ± 5.4% as listed in Table 2.

3.2. Characterization of alginate microgels loaded with PLGA NPs

The drug-loaded NPs were then encapsulated in the alginate microgels. The alginate-based microgel was prepared using a one-step process with a high-voltage electro-spraying system [23]. The resulted NPs encapsulated alginate microgels showed a good spherical geometry as evidenced by SEM (Fig. 2B). The average diameters of microgels encapsulated with DOX PLGA NPs and CIF PLGA NPs were 398.8 ± 18.0 and 402.1 ± 15.2 μm, respectively (Fig. 2B, Table 1). The successful encapsulation of drug-loaded PLGA NPs by the alginate microgels was further validated by the LSCM. As demonstrated in Fig. 2C, DOX-formulated PLGA NPs homogeneously distributed in the FITC-labeled alginate microgels.

3.3. Characterization of LGFU lens

The time-domain waveform at the focal distance (12.3 mm) showed an asymmetric bi-polar waveform (190% higher positive amplitude than negative amplitude, Fig. 3B). The LGFU transducer exhibited a −6 dB focal spot size of 400 μm in lateral and 3.8 mm in axial directions. The center frequency and −6 dB fractional bandwidth at the frequency spectrum are 14.5 MHz and 153%, respectively. The pressure output amplitudes at the focal spot were indirectly characterized for the laser energy ranging from 2 to 18 mJ. The corresponding peak-to-peak pressure output with 18 mJ laser input is 22.5 MPa (Fig. 3C). The negative pressure output with the maximum laser energy used in this work (18 mJ) is about −8 MPa.

3.4. Drug release from microgels promoted by LGFU

The promoted drug release behavior triggered by LGFU was evaluated in the PBS solution (pH = 7.4) at 37 °C. Although we observed a scattered laser light from the glass-concave lens during the LGFU treatment (Fig. 3A), the scattered laser energy at the test tube position was below the lower-limit of the laser energy meter (100 nJ), suggesting that the scattered light was negligible. In order to explicate the major mechanism for the enhanced release, a control sample for suppression of cavitation was tested by using a degassed buffer (Fig. 4A). The released DOX concentration in the degassed PBS solution was reduced by 44%, indicating that the cavitation induced by the single-pulsed photoacoustic waves is a major cause of the promoted drug release by LGFU [6].

At the focal point, the DOX concentration in the treated sample was 3.2 fold that of the samples were 3 mm away (in the axial direction) from the focal point (Fig. 4B). Fig. 4C and D shows that the release of DOX from microgels was promoted when increasing the laser energy and the treatment duration. In comparison with the passive release, a maximum of 3-fold of DOX release concentration was achieved with the laser input condition of 18 mJ (the corresponding peak-to-peak pressure output of 22.5 MPa) and 5 min treatment duration. However, no detectable temperature shift was observed during this treatment. Collectively, these results indicated that laser-generated pulsed waves were able to trigger the release of drug, which was passively released from NPs and temporarily stored in the microgels. Based on the preliminary experiments, the 18 mJ-laser input and 30 s treatment duration were selected as treatment conditions for the further tests. The daily experimental result exhibited a steadily increased release profile for both DOX (Fig. 5A) and CIF (Fig. 6A).

3.5. Anti-proliferation and inhibition of cancer cell spheroid growth tests

The anti-proliferation capability of the released drug triggered by LGFU from DOX-formulated microgels was evaluated on HeLa cells using MTT assay. As shown in Fig. 5B, daily addition of medium collected from samples after LGFU treatment, at day 3, day 5 and day 7 exhibited much higher toxicity when compared with control groups treated by DOX-contained medium associated with the passive release from the DOX-formulated microgels, indicating enhanced anticancer efficacy after administration by LGFU.

The tumor spheroid provides an effective tool to study the antitumor efficacy of the LGFU promoted drug release from DOX-formulated alginate microgels [24]. In this study, we utilized the HeLa tumor spheroids to evaluate the inhibition of HeLa spheroid growth for one week with the daily addition of 50 μL solution collected from DOX-formulated alginate microgels after LGFU treatment and daily addition of 50 μL solution collected from samples without treatment. As shown in Fig. 5C and D, the HeLa spheroid treated with DMEM kept growing and became more compact, whereas the HeLa spheroid exposed to DOX-contained medium passively released from sample exhibited apoptosis of marginal cells and reduction in sizes. In comparison, the spheroids treated with medium collected from samples after LGFU treatment exhibited the smallest size with loose intercellular junctions and lost the three-dimensional (3D) structure at day 7. These results further substantiated that LGFU can effectively promote drug release from DOX-formulated microgels, which significantly inhibited growth of spheroids.

3.6. Antibacterial activities

Bactericidal effects of released drug triggered by LGFU from CIF-formulated microgels were evaluated against *E. coli* (gram negative) using a standard agar disk diffusion method [25]. The daily experiment result exhibited a steady increase in the CIF cumulative release profile (Fig. 6A). After a 7-day treatment with LGFU, the cumulated CIF concentration showed approximately 2.5-fold increase compared to the concentration from the passive release mechanism. Fig. 6B and C elucidated the inhibition zones of sample with and without treated by LGFU against *E. coli*. The resulting inhibition zones at each pre-determined time point, after consecutive treatment of 3 days, 5 days and 7 days, exhibited superior antibacterial activities after LGFU treatment, with significantly larger inhibition zone sizes than that of without LGFU treatment.

4. Conclusion

In summary, we have developed a LGFU-triggered drug delivery system for spatiotemporally remote control of drug release. Alginate microgels integrated with drug-loaded NPs were specifically constructed to achieve promoted drug release, mainly based on the cavitation effect. The *in vitro* anticancer and antibacterial study reported here provides guidelines for further *in vivo* investigation and potentially clinical uses. For example, the LGFU lens can be customized based on the diagnostic information of the targeted tumor; the penetration depth and focal spot size are easily manipulated by designing the lens size, radius of curvature, and thickness of thermal expansion layer. This system can also be extended to the intravascular drug delivery by integrating optical-fibers with microlens at a microcatheter for precise drug-injection and promoted release.

Acknowledgments

This work was supported by the grant from NC TraCS, NIH's Clinical and Translational Science Awards (CTSA) at UNC-CH (1UL1TR001111), the NC State Faculty Research and Professional Development Award, and the start-up package from the Joint BME Department of UNC-CH and NC State to Z.G. The authors thank Dr. Tiegang Fang for assistance in equipment usage.

References

1. Mura S, Nicolas J, Couvreur P. Stimuli-responsive nanocarriers for drug delivery. Nat Mater. 2013; 12:991–1003. [PubMed: 24150417]
2. Lu Y, Sun W, Gu Z. Stimuli-responsive nanomaterials for therapeutic protein delivery. J Control Release. 2014; 194:1–19. [PubMed: 25151983]
3. Timko BP, Dvir T, Kohane DS. Remotely triggerable drug delivery systems. Adv Mater. 2010; 22:4925–4943. [PubMed: 20818618]
4. Ganta S, Devalapally H, Shahiwala A, Amiji M. A review of stimuli-responsive nanocarriers for drug and gene delivery. J Control Release. 2008; 126:187–204. [PubMed: 18261822]
5. Wang Y, Shim MS, Levinson NS, Sung HW, Xia Y. Stimuli-responsive materials for controlled release of theranostic agents. Adv Funct Mater. 2014; 24:4206–4220. [PubMed: 25477774]
6. Di J, Price J, Gu X, Jiang X, Jing Y, Gu Z. Ultrasound-triggered regulation of blood glucose levels using injectable nano-network. Adv Healthcare Mater. 2014; 3:811–816.
7. Pitt WG, Husseini GA, Staples BJ. Ultrasonic drug delivery—a general review. Expert Opin Drug Deliv. 2004; 1:37–56. [PubMed: 16296719]

8. Chen H, Hwang JH. Ultrasound-targeted microbubble destruction for chemothera-peutic drug delivery to solid tumors. J Ther Ultrasound. 2013; 1:1–10. [PubMed: 24761222]
9. Dromi S, Frenkel V, Luk A, Traughber B, Angstadt M, Bur M, Poff J, Xie J, Libutti SK, Li KC. Pulsed-high intensity focused ultrasound and low temperature-sensitive liposomes for enhanced targeted drug delivery and antitumor effect. Clin Cancer Res. 2007; 13:2722–2727. [PubMed: 17473205]
10. Ng KY, Liu Y. Therapeutic ultrasound: its application in drug delivery. Med Res Rev. 2002; 22:204–223. [PubMed: 11857639]
11. Mitragotri S, Blankschtein D, Langer R. Ultrasound-mediated transdermal protein delivery. Science. 1995; 269:850–853. [PubMed: 7638603]
12. Martin KH, Dayton PA. Current status and prospects for microbubbles in ultrasound theranostics. Wiley Interdiscip Rev Nanomed Nanobiotechnol. 2013; 5:329–345. [PubMed: 23504911]
13. Kost J, Leong K, Langer R. Ultrasound-enhanced polymer degradation and release of incorporated substances. Proc Natl Acad Sci U S A. 1989; 86:7663–7666. [PubMed: 2813349]
14. Huebsch N, Kearney CJ, Zhao X, Kim J, Cezar CA, Suo Z, Mooney DJ. Ultrasound-triggered disruption and self-healing of reversibly cross-linked hydrogels for drug delivery and enhanced chemotherapy. Proc Natl Acad Sci U S A. 2014; 111:9762–9767. [PubMed: 24961369]
15. Baac HW, Ok JG, Maxwell A, Lee K-T, Chen Y-C, Hart AJ, Xu Z, Yoon E, Guo LJ. Carbon-nanotube optoacoustic lens for focused ultrasound generation and high-precision targeted therapy. Sci Rep. 2012; 2
16. Lee T, Baac HW, Ok JG, Youn HS, Guo LJ. Controlled generation of single microbubble at solid surfaces by a nanosecond pressure pulse. Phys Rev Appl. 2014; 2:024007.
17. Hsieh BY, Kim J, Zhu J, Li S, Zhang X, Jiang X. A laser ultrasound transducer using carbon nanofibers–polydimethylsiloxane composite thin film. Appl Phys Lett. 2015; 106:021902.
18. Zhu H, Srivastava R, Brown JQ, McShane MJ. Combined physical and chemical immobilization of glucose oxidase in alginate microspheres improves stability of encapsulation and activity. Bioconjug Chem. 2005; 16:1451–1458. [PubMed: 16287241]
19. Di, J.; Yao, S.; Ye, Y.; Cui, Z.; Yu, J.; Ghosh, TK.; Zhu, Y.; Gu, Z. Stretch-triggered drug delivery from wearable elastomers containing therapeutic depots. ACS Nano. 2015. http://dx.doi.org/10.1021/acsnano.5b03975
20. Tong L, Lim C, Li Y. Generation of high-intensity focused ultrasound by carbon nanotube opto-acoustic lens. J Appl Mech T ASME. 2014; 81:081014.
21. Hu Q, Gao X, Gu G, Kang T, Tu Y, Liu Z, Song Q, Yao L, Pang Z, Jiang X. Glioma therapy using tumor homing and penetrating peptide-functionalized PEG–PLA nanoparticles loaded with paclitaxel. Biomaterials. 2013; 34:5640–5650. [PubMed: 23639530]
22. Gu Z, Aimetti AA, Wang Q, Dang TT, Zhang Y, Veiseh O, Cheng H, Langer RS, Anderson DG. Injectable nano-network for glucose-mediated insulin delivery. ACS Nano. 2013; 7:4194–4201. [PubMed: 23638642]
23. Gu Z, Dang TT, Ma M, Tang BC, Cheng H, Jiang S, Dong Y, Zhang Y, Anderson DG. Glucose-responsive microgels integrated with enzyme nanocapsules for closed-loop insulin delivery. ACS Nano. 2013; 7:6758–6766. [PubMed: 23834678]
24. Minchinton AI, Tannock IF. Drug penetration in solid tumours. Nat Rev Cancer. 2006; 6:583–592. [PubMed: 16862189]
25. Fayaz AM, Balaji K, Girilal M, Yadav R, Kalaichelvan PT, Venketesan R. Biogenic synthesis of silver nanoparticles and their synergistic effect with antibiotics: a study against gram-positive and gram-negative bacteria. Nanomed Nanotechnol Biol Med. 2010; 6:103–109.

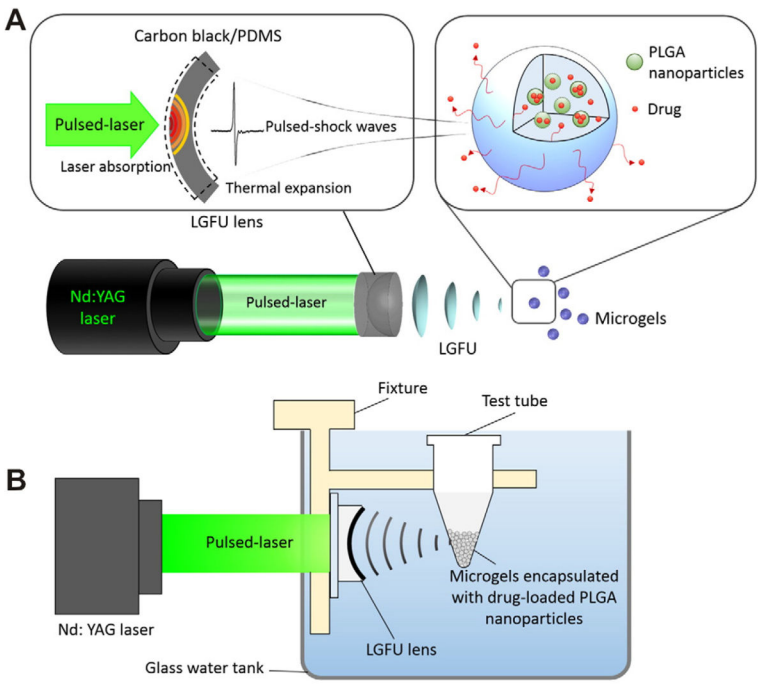

Fig. 1.

Schematic of the laser-generated-focused ultrasound-mediated drug delivery. (A) Once the carbon black/PDMS LGFU transducer is excited by the pulsed-laser, the absorbed laser energy causes rapid heat-transfer and simultaneous thermal expansion of the LGFU lens. The laser-generated pulsed waves can promote the drug-release efficiency by cavitation effects and oscillation of the microgels' shells. (B) Schematic of the experimental apparatus; a customized fixture is used to maintain the consistent position of the test tube at the focal spot.

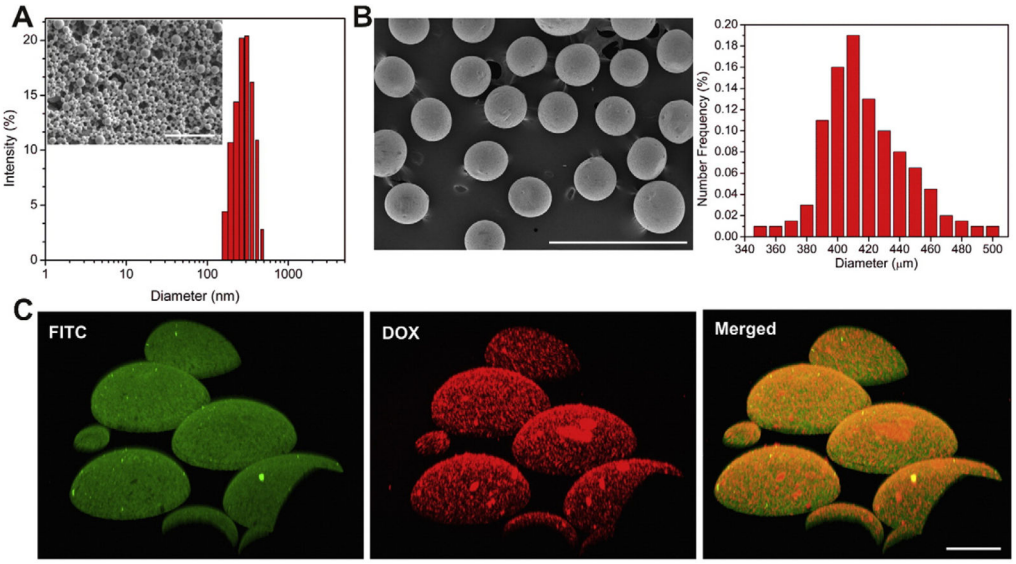

Fig. 2.

Characterizations of the DOX-loaded PLGA NPs, alginate microgels loaded with PLGA NPs and characterizations of laser-generated-focused ultrasound. (A) SEM image of the PLGA NPs (scale bar: 1 μm) (inset) and the polydispersity intensity as a function of the PLGA NPs diameter measured by dynamic light scattering (DLS). (B) SEM image (left) and size distribution (right) of alginate microgels loaded with PLGA NPs. Scale bar: 1 mm. (C) Laser scanning confocal microscopy (LSCM) image of the FITC-tagged alginate microgels' shell; the DOX loaded PLGA NPs, and the merged image of microparticles with DOX loaded NPs. Scale bar: 100 μm.

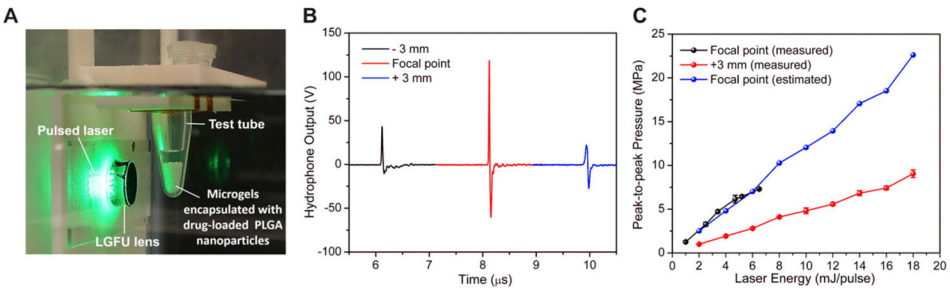

Fig. 3.

(A) A customized fixture for positioning the test tube at focal point. (B) Time-domain waveforms at the focal distance (12.3 mm) and ±3 mm away (along the axial direction) from the focal distance. (C) Characterized pressure output amplitudes versus laser energy. Actual pressure outputs at the focal distance are indirectly determined in accordance with the measured pressure outputs at 3 mm away. Data represents mean ± SD (n = 3).

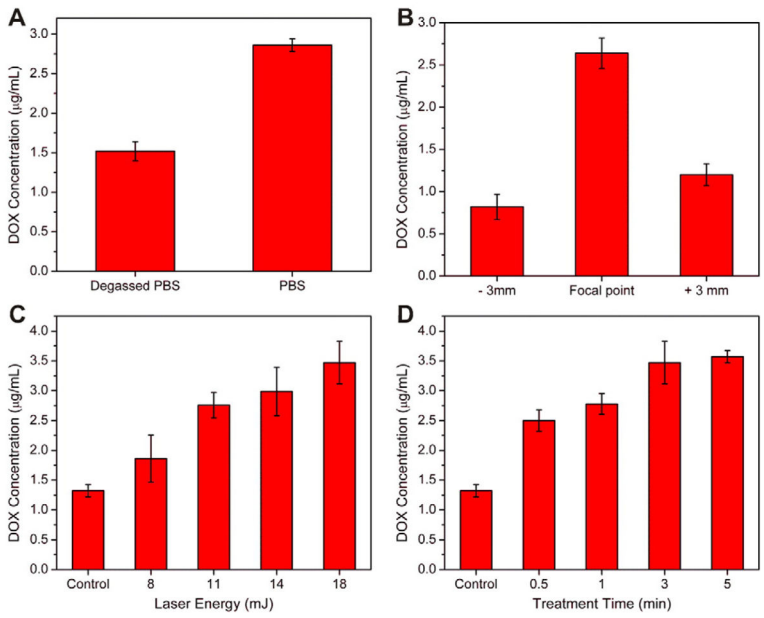

Fig. 4.

The promoted drug release triggered by the LGFU system. (A) DOX concentration comparison between PBS and degassed PBS (18 mJ, 30 s). (B) DOX-release amount at the focal point and 3 mm away (along the axial direction) from the focal point; treated by 18 mJ excitation during 30 s. (C and D) The release concentration upon variation of LGFU parameters: (C) input energy changes at a fixed duration of 3 min; (D) treatment duration changes at a fixed laser energy of 18 mJ. Data represents mean ± SD (n = 3).

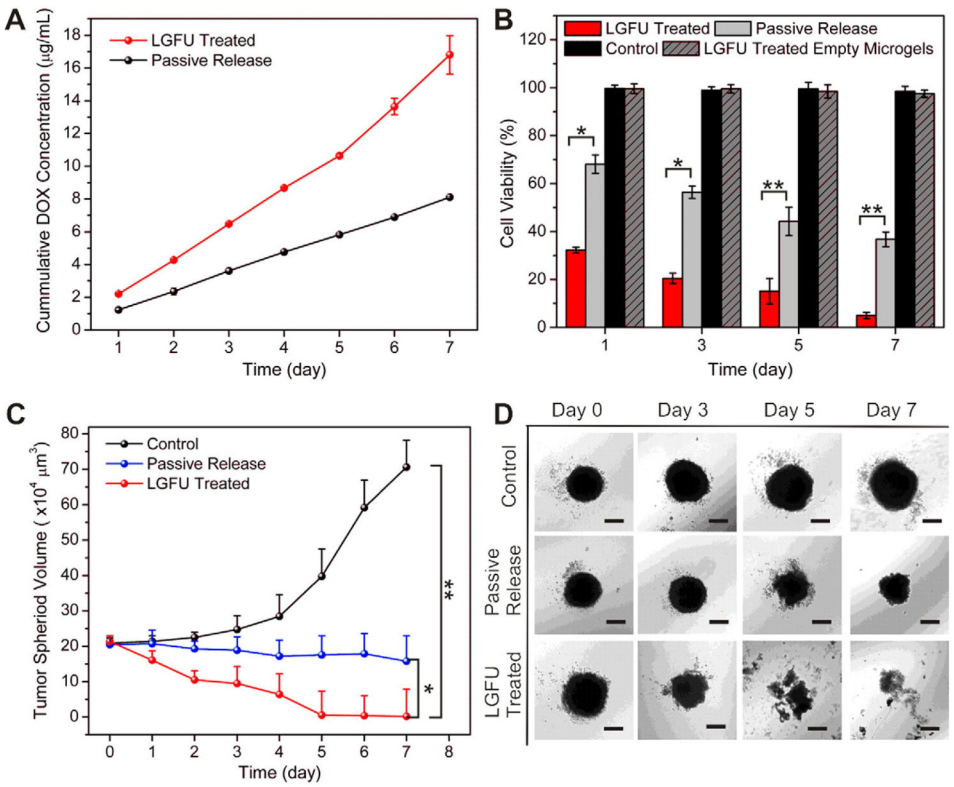

Fig. 5.

LGFU-induced anticancer effects *in vitro*. (A) The cumulative concentration of released DOX after 30 s treatment with LGFU (18 mJ) and passively released DOX without LGFU treatment. (B) Cell viability of HeLa cells treated by solutions from DOX-formulated microgels after 30 s treatment with LGFU (18 mJ) and passive released DOX. (C and D) Normalized HeLa tumor spheroid sizes and morphologies at day 0, day 3, day 5 and day 7 after treated with solutions associated with DOX-formulated microgels treated by LGFU, formulations without LGFU treatment (passive release) and PBS (control). Scale bars: 100 μm. Data represents mean ± SD ($n = 3$). $^{*}P < 0.05$ (t-test), $^{**}P < 0.01$ (two-tailed Student's *t*-test).

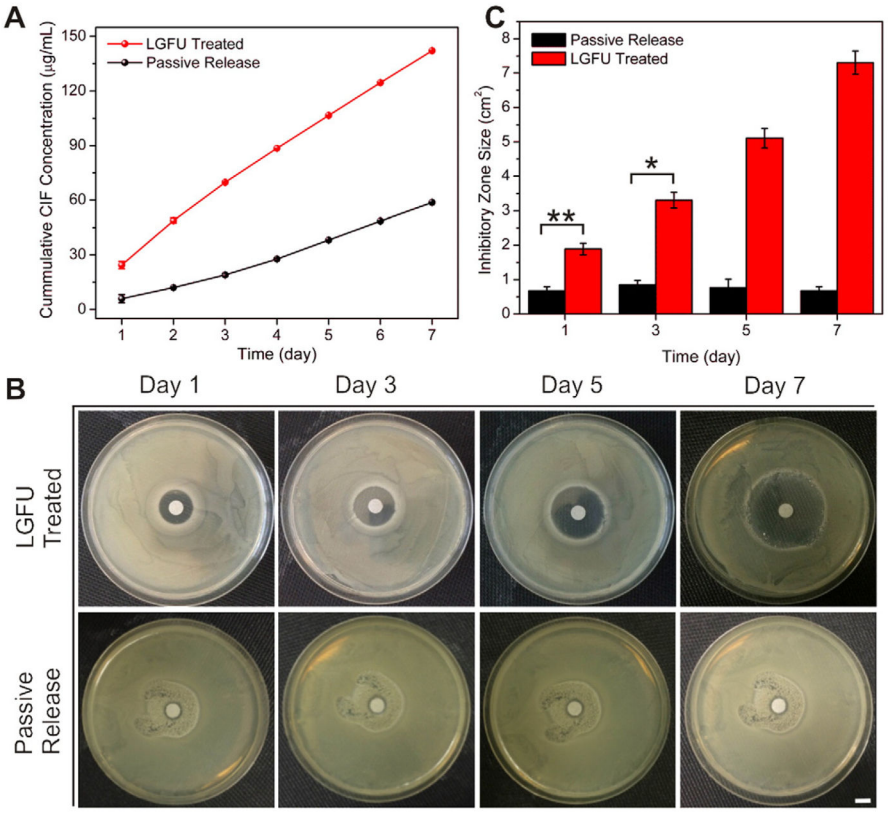

Fig. 6.

In vitro ciprofloxacin (CIF) release from microgels encapsulated with CIF loaded PLGA NPs and its bactericidal applications. (A) CIF cumulative release amount after 30 s treatment with LGFU (18 mJ), and passively released CIF without LGFU treatment. (B) Pictures of the diameter of the inhibitory zone produced around the filter-paper disks after incubating for 24 h at 37 °C. 50 μL of samples after LGFU treatment were applied daily to the sterilized filter-paper disks with a diameter of 5 mm. The CIF diffused from the filter-paper disks to inhibit *E. coli* growth. (C) The diameter of the inhibitory zone produced around the filter-paper disks measured after incubation at 37 °C for 24 h. Scale bar: 5 mm. Data represents mean ± SD ($n = 3$). $^{*}P < 0.05$ (*t*-test), $^{**}P < 0.01$ (two-tailed Student's *t*-test).

Table 1

Physical characterization of drug loaded PLGA NPs and alginate microgels.

	DOX	CIF
NPs' mean size (mean ± SD, nm)	249.2 ± 10. 1	259.9 ± 17.2
NPs' zeta potential (mV)	−67.2 ± 5.1	−65.5 ± 4.3
Microgels' mean size (mean ± SD, μm)	398.8 ± 18.0	402.1 ± 15.2

Table 2

Drug loading capacity (LC) and encapsulation efficiency (EE) of PLGA NPs encapsulated with DOX and CIF.

	NPs (DOX)	NPs (CIF)
LC (%)	3.3 ± 0.2	3.5 ± 0.3
EE (%)	47.3 ± 7.1	44.3 ± 5.4